Chapter 1

Introduction

1.1 A brief history of X-ray astronomy

X-rays are high-energy electromagnetic waves which spread over electromagnetic spectrum in the wavelength range (1-100 Å) . The energy of X-rays lies between $\sim$0.12-120 keV. X-ray was discovered by W. C. Röntgen in 1895 when he observed a faint glow produced on a fluorescent screen due to some unknown rays coming from the discharge tube. X-rays being high energy radiation can ionize atoms. The interaction of X-rays with matter can cause Compton effect, photo-electric effect, Thomson scattering etc. X-ray are generally produced by the colliding a highly accelerated electrons with a tungsten, the electrons coming from the cathode of a vacuum tube are accelerated by applying high voltage of an order of keV.

There are plenty of X-ray sources in our universe but Earth's atmosphere is opaque to high energy radiations like UV, X-rays and gamma rays. So the ground based observatories which can detect optical and radio waves cannot detect these high energy radiation coming from outer space. So X-ray detector must be placed above the atmosphere and this is done with the the help of rocket flights and balloons. The search for the X-ray sources from outer space began in 1948. In September 1949, a team of researchers from US Naval Research

Laboratory detected weak X-rays coming from the hot corona of sun using German V2 sounding rocket launched in January 28, 1949 from New Mexico. A set of Geiger counters was placed at the nose cone of the rocket. It was after more than a decade a first celestial X-ray source outside the solar system Sco X-1 in the constellation of Scorpius was discovered in 1962 by a team led by Riccardo Giacconi using *Aerobee 150* sounding rocket carrying a small X-ray detector (Giacconi *et al.*, 1962). The presence of galactic X-ray sources was further supported by the two rocket experiments performed in October 1962 and June 1963 from the White Sands Missile Range, New Mexico (Gursky *et al.*, 1963). In this decade numerous X-ray sources were discovered using rocket flights. The first X-ray imaging telescope was made by team led by Riccardo Giacconi at American Science and Engineering in Cambridge, MA which was sent into space on a small sounding rocket in 1963 and was used to make crude images of the hot spots present in sun's atmosphere. The first satellite dedicated to X-ray astronomy was *Uhuru* (Giacconi *et al.*, 1971), launched on December 1970 and was operational for two years. It was also known as Small Astronomy Satellite 1 *(SAS-1)* or Explorer 42. The fourth Uhuru catalog consists of detail of position and intensities of 339 X-ray sources (Forman *et al.*, 1978). After *Uhuru* X-ray satellites namely *SAS 2, Ariel, SAS 3, HEA0-1, HEAO-2* and *HEAO-3* were also launched in this decade. The first focusing X-ray telescope was the Apollo Telescope Mount aboard Skylab, US first space station which was launched in May 1973. The first fully imaging X-ray telescope was *HEAO-2* or *Einstein* observatory which was launched in November 1978. In 1980's X-ray satellite like *EXOSAT* and *Ginga* were launched, while in 1990's important missions like *ROSAT, ASCA, RXTE, BeppoSAX, XMM* and *Chandra* were launched. The *RXTE* was used to study rapid time variability of X-ray emitted from sources over a wide energy range. The imaging capacity of the *Chandra* observatory is excellent, it is able to detect X-ray sources twice as far away detected by other observatories, which can also produce images five times more prominent. During the first decade of 21^{st} century, X-ray

observatory like *Suzaku, Swift, INTEGRAL, MAXI, AGILE* and *Fermi* have been launched, except *Suzaku* all of them are operational till date. The other mission which are under operational at present are *Chandra, NuSTAR* and *AstroSat*, the last two observatories were launched in 2012 and 2015 respectively.

1.2 Compact Objects

Compact objects are astronomical objects which are very dense star compared to a typical star. They are stellar remnants as they are formed at the end stage of stellar evolution. There are three types of compact objects - white dwarf, neutron star and black hole. The compact objects are formed as a result of gravitational collapse when the radiation pressure due to nuclear fusion in the star is no longer able to hold the gravitational pressure, as a result a compact core of the star is left behind. In that case the inward gravitational pressure is balanced by the degenerate pressure of fermions, may be electron or neutron. The type of the compact object formed depends on the mass of the proto-star.

- **White dwarfs** - These type of compact objects are formed by the gravitational collapse when the initial mass of the proto-star is less than $8M_{\odot}$, where $M_{\odot}$ is the solar mass. They are found to have small radii and emit thermal energy with the effective temperature greater than normal stars but with low luminosities. The gravitational collapse tears out the electrons from the atom and the degenerate pressure which can be measured due to Pauli's exclusion principle now halts the further collapse of the star. A new star is born which is white dwarf. It was Chandrasekhar who showed that the maximum mass of a white dwarf is $1.24M_{\odot}$. Adams (1915) discovered that the spectral type of Sirius B is similar to its normal companion star Sirius. From the spectral type the estimated effective temperature of Sirius B was 8000 K and from the luminosity the

predicted radius was about 18800 km. Adams (1915) also determined that its density to be 5×10^4 g cm^{-3}. However these prediction are affected because of presence of its companion Sirius. The recent measured temperature of Sirius B is about 27000 K with density about 3×10^6 g cm^{-3} and radius about four times smaller than predicted earlier. Einstein in 1907 theoretically found that the presence of such highly dense compact object creates strong gravitational field around it which causes redshift of light, Adams (1925) detected the redshift equivalent to $\sim$ 19 km s^{-1} for Sirius B, which confirmed that Sirius B is a very high dense object. The magnetic field of the white dwarfs lies between 10^6 to 10^9 G (Schmidt, 1989). The average mass of white dwarf is 0.57M$_\odot$ (Kepler *et al.*, 2007), where as the minimum estimate mass is 0.17M$_\odot$ (Kilic *et al.*, 2007) and maximum being 1.33M$_\odot$ (Kepler *et al.*, 2007). The mean density of white dwarf is around 10^6 gcm^{-3} and radius about $\sim$7000 km.

The cooling of the white dwarf occurs through the loss of the thermal energy in the form of the radiation. For Kramers' law opacity in the envelope the cooling time (t_{cool}) depends on the luminosity such that $t_{cool}\ \alpha\ L^{-5/7}$ which is also inversely proportional to the mean atomic weight of the interior ions (van Horn, 1971). Other than the thermal cooling the processes responsible for the cooling of white dwarfs are due to neutrino cooling, crystallization and Debye cooling. During the initial and final phases of the evolution of white dwarfs, the degeneracy pressure is not equal everywhere but there exist regions of low degeneracy pressure where contraction still takes place. So there will be release of gravitational energy in the form of radiation which contributes to their observed luminosity. The cooling age of the faintest white dwarf is about 9×10^9 years and the life time of its progenitor is about 0.3×10^9 which together gives an age of the galactic disk to be about 9.3×10^9. Hot white dwarfs are the

source of UV and soft X-rays. It is known that a white dwarf in binary system with a companion might be a source of X-rays.

- **Neutron star** - In 1934 Baade & Zwicky proposed the formation of a compact object made up of neutrons during supernovae explosion. Oppenheimer & Volkoff in 1939 were first to calculate masses and radii of the neutron stars by assuming that they are composed of neutrons at high density which behave like an ideal gas. They predicted that the maximum mass for neutron stars to be in equilibrium was $\sim 0.7M_{\odot}$, above this the core will collapse further. However this mass limit was below the Chandrasekhar limit of $1.4M_{\odot}$ for white dwarf, the reason behind this was that they did not take the neutron-neutron interaction into account (Ghosh, 2006). By the inclusion of the neutron-neutron interaction the Oppenheimer & Volkoff limit raise to $\sim 2M_{\odot}$ (Cameron, 1959). It was in 1962 when first X-ray source outside solar system was discovered, which brought a wide interest in astronomers about neutron stars as the possible X-ray sources in the sky. X-rays were thought to be originated from cooling of the hot neutron stars. Another very important event was the discovery of quasar in 1963 by Schmidt that raised further interest in exploring neutron stars. The large redshifts of the spectral lines of quasars were thought to be due to large gravitational field of neutron star. However this concept was soon abandoned as the largest observed redshift from the quasars during that time is found to exceed the maximum redshift from the neutron star surface. With the discovery of pulsar in 1967 (Hewish *et al.*, 1968), Gold (1968) proposed that pulsars are nothing but a rotating neutron star. Further evidence for the existence of the neutron star came from the discovery of X-ray pulsars by UHURU in 1971, which were thought to be a binary system between neutron star and a normal companion, where the neutron star accretes matter from the companion.

The mass of the neutron stars were determined using the optical and X-ray observations of some X-ray pulsars. Neutron stars are believed to be formed if the mass of the progenitor is greater than $8M_{\odot}$. In a neutron star the neutron degeneracy pressure balances the star from further collapse due to gravitation. If a star exceeds the theoretical mass limit $3.3M_{\odot}$ (TOV limit) it will further collapse to be a black hole. However, it is known that the mass of the neutron star lies between 1.17-2.0$M_{\odot}$ and radius in 9.9-11.2 km range (Özel and Freire, 2016). The density of a typical neutron star is of the order of 10^{14} g cm^{-3} which is about nuclear density. The magnetic field of the neutron star is found to lie in the range 10^{8}-10^{15} G.

- **Black hole** - In 1795 Laplace using Newtonian gravity discussed the possibility of existence of compact objects having gravitational field so strong that even light cannot escape from their surfaces. In 1915, Albert Einstein proposed general theory of relativity and soon after this Karl Schwarzschild in 1916 was that first to obtain the solution of Einstein field equations for the gravitational field around the spherical object which is the popular vacuum solution. The solution describes a uncharged non-rotating black hole. Hans Reissner in 1916 gave a solution for a charged spherically symmetric non-rotating black hole. The solution describing rotating uncharged black hole was given by Roy Kerr in 1963. Eddington in 1935 discussed that if Chandrasekhar's mass limit is true then the stellar core having mass greater than the limit will go on contracting and radiating until the radius of the core becomes few km and its gravitational field is strong enough to hold the light. In 1939 the formation of the black hole was first demonstrated by Oppenheimer and Snyder when they observed that a homogeneous sphere of pressureless gas becomes cut off from communication from the rest of the universe when it is allowed to collapse in general relativity.

Yakov Zel'dovich and Edwin Salpeter in 1964 independently proposed that quasars were supermassive black holes powered by matter accreting around them. In 1971 astronomers found the massive companion of the X-ray source Cygnus X-1 and estimated the mass of the compact object by studying the motion of the companion (Bolton, 1972; Webster and Murdin, 1972). The mass of the compact object in Cygnus X-1 exceeded the maximum mass of the neutron star and was considered as first the stellar black hole candidate. Today it has been accepted that there are number of black hole candidates in binaries and supermassive black holes that exist at that of the galaxies. Classically black holes are regions in the spacetime that cannot communicate with the rest of the universe. The boundary of this region is called event horizon (Shapiro and Teukolsky, 1983). Inside the event horizon there exist a singularity where laws of physics is not valid. It is now understand that black holes are defined by mass M, electric charge Q and spin angular momentum J in reality.

1.2.1 X-ray Binaries

X-ray binaries (XRBs) are binary system between a compact object and a companion which can be a normal star or another compact object which is a source of X-rays. Depending upon the type of compact objects, XRBs are divided into three groups viz - (1) Black hole binaries (2) Neutron star X-ray binaries (3) White dwarf X-ray binaries. They are the major sources of extraterrestrial X-rays having luminosities in the range of 10^{33}-10^{39} erg s^{-1}. Depending on the mass of the companion star, Neutron star and black hole X-ray binaries can be of two types- High Mass X-ray Binaries (HMXBs) and Low Mass X-ray Binaries (LMXBs). For HMXBs, the mass of the companion is $\geq 10M_{\odot}$ and for LMXBs the companion mass $M < 2M_{\odot}$. The optical companion of HMXBs is type O or B star where as LMXBs have companion of spectral type after A. The orbital period of HMXBs

varies from few days to a year but in case of LMXBs it ranges from less than a hour to days. Accretion disk is small or absent in HMXBs where as in the case of LMXBs it is always present. Neutron star (NS) HMXBs shows pulsation where as in NS LMXBs pulsation is seen only in some cases. The magnetic field of a NS in HMXBs is of the order of 10^{12} G and in LMXBs its about 10^8 G. HMXBs are comparatively young (age <10^7 years) compared to LMXBs having age $\sim 10^9$ years. HMXBs have hard X-ray spectra with $kT \geq 15$ keV where as LMXBs have soft X-ray spectra ($kT \sim 2$ keV) (Jaisawal, 2016). NS HMXBs are further classified into two subgroups - (i) Be/X-ray binaries (BeXBs) and (ii) Super-Giant X-ray Binaries (SGXB), whereas NS LMXBs are divided into two subgroups - (i) Atoll and (ii) Z-sources. Be/X-ray binaries have an optical companion which can be dwarf, subgiant or giant OBe star with luminosity class between III-V. SGXBs have a supergiant companion having luminosity I or II and are bright and persistent. BeXBs are mostly transient in nature having eccentricity, e$\geq$ 3 (Reig, 2011). They are observable during an outburst, where outbursts may be a Type I or Type II. Type I outbursts are frequent but Type II outbursts are rare and giant. There are few persistent BeXB rotating slowly ($P > 200$ s) and orbital period $P_{orb} > 200$ days (Reig, 2011). Black hole (BH) X-ray binaries can be persistent or transient in nature. BH HMXBs are persistent in nature but BH LMXBs are mostly transient. The schematic classification of X-ray binaries is shown in Fig. 1.1. The basic process which is responsible for the emission of the X-rays by XRBs is accretion of matter from the companion to the compact objects. There are three ways through which the accretion of matter onto the compact objects occurs, namely (a) Roche-lobe overflow, (b) stellar wind accretion and (c) Be-disk accretion. Accretion in NS LMXBs and BeXBs occurs through Roche-lobe overflow where as in SGXBs there are three disc-fed X-ray binaries where mass transfer occurs through Roche-lobe overflow and there are few tens of SGXBs where mass transfer occurs through stellar wind. In case of black hole, mass accretion in persistent BH HMXB occurs through stellar wind where as

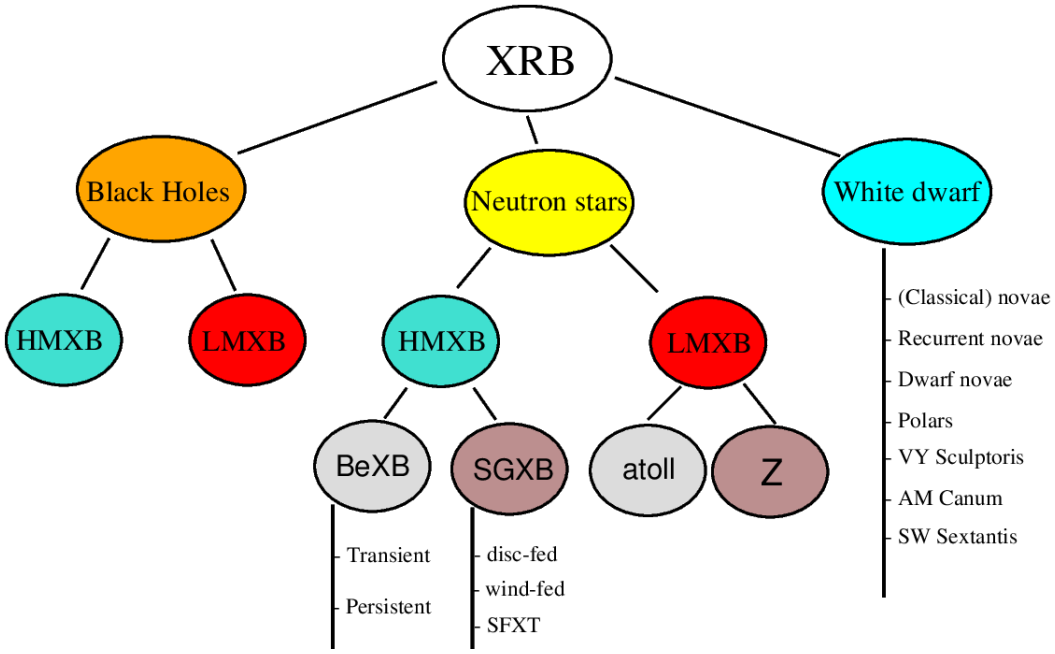

Fig. 1.1 Classification of X-ray binaries. Image courtesy Reig (2011).

in BH LMXB the mass transfer occurs through Roche-lobe overflow. However it is the nature of the compact object which determines the properties of the emitted X-rays.

1.3 Theory of Accretion

In a binary system accretion is a process which powers the most luminous objects in the universe. The gravitational potential energy of the accreting matter in binary system is converted into kinetic energy which subsequently converted into radiation. It is an efficient process for converting the gravitational potential energy into radiation. For understanding accretion theoretically we consider a particle of mass (m) being accreted onto the surface of a body of mass (M) and radius (R), then the gravitation potential energy released will be,

$$E = \frac{GMm}{R} \tag{1.1}$$

where G is the Newton's gravitational constant. Assuming the accreting body to be a neutron star of mass equal to solar mass $M_{\odot}$ and radius $R \sim 10$ km, the energy released E is about 10^{20} erg for $m = 1$ gm. The maximum energy extracted in conversion of unit mass of hydrogen into helium by the process of nuclear fusion is 6×10^{18} erg, which is about 20 times smaller than the energy released during accretion (Frank *et al.*, 1992). The energy released during accretion depends on compactness i.e. M/R ratio of the accreting object, so the efficiency of energy released by accretion will be greater if the object is highly compact. So accretion is efficient way through which energy is released in the case of black holes and neutron star.

The luminosity produced by the accretion of matter onto compact object, which is known as accretion luminosity is given by,

$$L_{acc} = \frac{GM\dot{M}}{R} \tag{1.2}$$

where $\dot{M}$ represents the mass accretion rate. However the total potential energy cannot be released out as the radiation. The efficiency of the accretion process is measured by a dimensionless quantity η, defined as

$$\eta = \frac{L_{acc}}{\dot{M}c^2}. \tag{1.3}$$

In this case for a neutron star of solar mass ($M_{\odot}$) the calculated efficiency is $\eta \sim 0.15$. From the eq.(1.2) we can see that the accretion luminosity (L_{acc}) of a given star is directly proportional to the mass accretion rate ($\dot{M}$). So higher the accretion rate higher is the accretion luminosity but there exists upper bound on the accretion luminosity above which the accretion can be halted. This upper limit of the accretion luminosity is known as the Eddington luminosity. To estimate this we consider a steady spherically symmetric accretion of matter, which consists of fully ionized hydrogen gas. Since the cross section of

the Thomson scattering is negligible in the case of proton, so it is the free electrons which experience the force due to radiation and latter undergoes Thomson scattering (Frank *et al.*, 1992). If S be the radiant energy flux and σ_T, the Thomson cross section then the radial force acting outward on each electron is given by σ_TS/c. The radiant energy flux (S) is related to luminosity (L) which is given by the relation S=L/4πR^2. The gravitational pull acting on the pair of electron and proton is $\frac{GMm_p+m_e)}{R^2} \cong \frac{GMm_p}{R^2}$, where m_p and m_e are proton and electron masses respectively. At Eddington limit the luminosity at which the force due to radiation and gravitation acting on the electron-proton pairs are in equilibrium, is given by

$$\frac{L_{Edd}}{4\pi R^2 c} = \frac{GMm_p}{R^2} \tag{1.4}$$

where c is the speed of light and for electron σ_T is equal to 6.6×10^{-22} cm^2. From the eq. (1.4) it is evident that the Eddington limit and the maximum mass accretion rate is given as,

$$L_{Edd} = \frac{4\pi GMm_p c}{\sigma_T} = 1.3\times10^{38}\frac{M}{M_\odot} erg^{-1}, \tag{1.5}$$

$$\dot{M} = \frac{4\pi Rm_p c}{\sigma_T} = 1.5\times10^{-8}\frac{R}{10^6}M_\odot^{-1}.$$

As the above limit is derived by assuming steady accretion onto a spherical geometry, so it is not valid in the case of non-steady accretion in a non-spherical geometry *e.g.* in the case of supernova explosion where the luminosity exceeds the limit. However, the above limiting value is not valid in the presence of higher nuclei other than hydrogen in the accreting material (Frank *et al.*, 1992; Pradhan, 2016). X-rays emitting from a compact

object are mainly due to the accretion of matter from a companion to the compact object. The different accretion mechanisms is discussed in the next section.

1.4 Accretion Mechanism

A binary system consists of two components primary star and secondary star, orbiting around their common center of mass. Before discussing the different accretion mechanisms we need to know about the different potential surfaces formed by the self-gravitational force of the stars and their mutual gravitational interactions. For a star having certain mass and radius spherical equipotential surfaces are formed around it. These equipotential surface no longer remain symmetric in the presence of a second star and gets distorted from the spherical symmetry. The effective gravitational potential (Roche potential) is then determined by the gravitational potential of the individual star and the centrifugal force due to the the motion of stars about the center of mass. The Roche potential ϕ_R is given by

$$\phi_R = -\frac{GM_1}{|r-r_1|} - \frac{GM_2}{|r-r_2|} - \frac{1}{2}(\omega \times r)^2 \tag{1.6}$$

where M_1, M_2 are the masses of two stars, r_1 and r_2 are the position vectors of the star centers. The first two term in the Roche potential represents the individual potentials on a test particle at distance r and in third term ω is the angular velocity of the binary system with respect to the inertial frame represented above. For mass ratio 0.2 the geometry of the equipotential surface is shown in Fig. 1.2. The points where the gradient of the Roche potential vanish are called Lagrangian points denoted by L_1, L_2, L_3, L_4, L_5 in Fig. 1.2. It is evident from the Fig. 1.2 that the three points L_1, L_2 and L_3 are lying on the line joining the centers of two stars where as L_4 and L_5 lying perpendicular to the line. The equipotential surfaces near the stars are almost spherical as it is dominated by the gravitational potential of the individual star but as one moves far away from the stars due

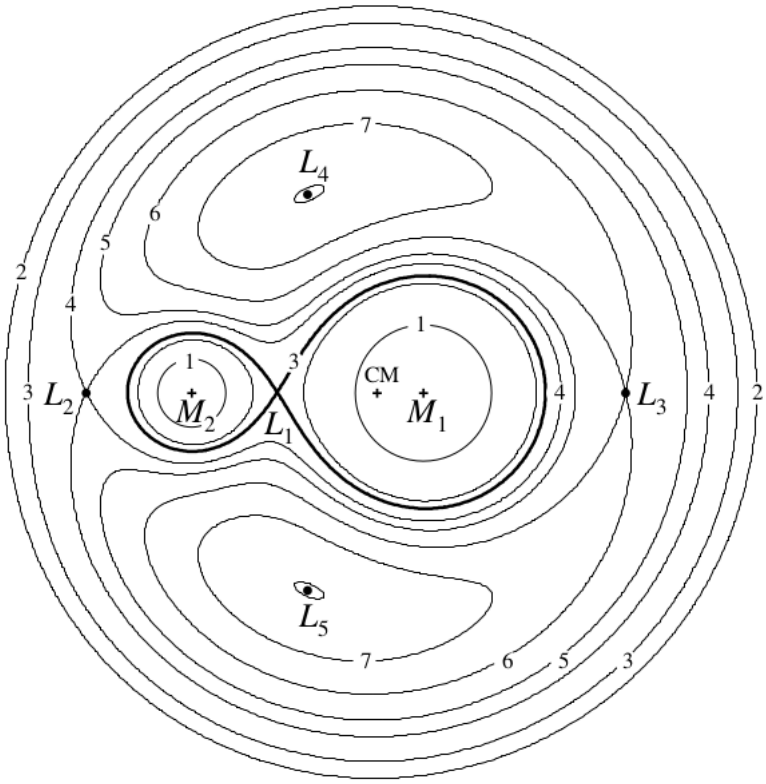

Fig. 1.2 Illustration of equipotential surfaces for binary system having mass ratio M_2/M_1=0.25. CM indicates center of mass where as L_1-L_5 indicate Lagrangian points. Equipotential surfaces are labelled by the numeral 1 to 7 in the increasing order of their magnitude. Image credit Frank *et al.* (1992)

.

to its tidal effect there is an elongation of the surface of the companion and centrifugal forces flatten them. The nearly circular region surrounding each star is known as Roche lobe. The lobes are connected with each other through an inner Lagrangian point L_1. The point L_1 is the saddle point which means that the mass in the vicinity of this point moves easily from one lobe to the another. Matter from the companion fills its Roche lobe and after that matter will escape into the Roche lobe of compact object through L_1. This type of mass transfer is known as Roche lobe overflow. In the following section we discuss about this type of mass transfer along with the other two processes namely, Stellar wind accretion and Be disk accretion .

1.4.1 Roche-lobe overflow

The binary system evolves with time and during the course of its evolution the separation between two stars decreases due to radial expansion of the companion star to the point where the gravitational pull of the compact object is sufficient enough to strip off it's outer layer or due to loss of orbital angular momentum of the system in the form of stellar wind or due to gravitational radiation. As the binary separation decreases, the size of the Roche lobes also decreases as a result matter from the Roche lobe of the companion flows into the Roche lobe of the compact object through the inner Lagrangian point L_1. This process of accretion is known as Roche-lobe overflow. As discussed earlier this type of mass flow is common in LMXBs. Matter from the companion is not accreted directly onto the compact object as it carries some angular momentum due to the rotation of companion. So the accreted matter spiral around the compact object in a circular orbit. Formation of accretion disk around the compact object occurs when the circularization radius (R_{cir}) is greater than the radius of accreting object. At the circularization radius the specific angular momentum (J) of the accreting matter becomes same as that in a circular orbit around the compact object. The circularization radius is given by,

$$R_{cir} = \frac{J^2}{GM} \tag{1.7}$$

where M is the mass of the compact object. The formation of disk begins at this radius. The accreting matter orbiting around the compact object starts losing its angular momentum which transfers due to viscous dissipation and moves inward into the orbit of smaller radius, thus forming an accretion disk. For a typical LMXB the circularization radius is given by

$$R_{cir} \geq 3.5 \times 10^9 M_C^{1/3} P_{hr}^{2/3} cm$$

where M_C is the mass of the companion in terms of solar mass and P_{hr} is the orbital period of binary in hours. Thus the circularization radius R_{cir}> 10^9 cm which is greater than the radius of the compact object thus the formation of the disk is very obvious in LMXBs, which is supported by observations.

1.4.2 Stellar Wind Accretion

Stellar wind accretion is common in close binary systems having early O or B type star and a compact object (neutron star or black hole). So stellar wind accretion occurs mostly in HMXBs. They are highly luminous object because of this X-ray sources was discovered first in these system. The early type stellar companion throws out matter in the form of stellar wind at the rate of 10^{-6}-10^{-5} $M_\odot$ yr^{-1} with a very high velocity (Frank *et al.*, 1992). The velocity of the stellar wind (v_w) is given as follow,

$$v_w(r) \sim v_{esc}(R_s) = \left(\frac{2GM_s}{R_s}\right)^{1/2} \tag{1.8}$$

where v_{esc} is the escape velocity at the surface of the star, M_s and R_s are the mass and radius of the star respectively. For the typical values of M_s and R_s the velocity of the stellar wind v_w is few thousand km s^{-1}. If v_n is the orbital velocity of the compact object about its companion then the relative velocity of the wind is v_{rel}=$(v_n^2 + v_w^2)^{1/2} \approx v_W$, as the velocity of the neutron star is relatively small compared to the wind velocity. As the wind passes close to the compact object it will make an angle $\beta \cong tan^{-1}(v_n/v_w)$ with the line of centers. If the kinetic energy of wind particles passing close to the compact object is less than the gravitational potential energy, then it will get captured and will be accreted by the compact object. The wind capture takes place in the cylindrical region along the wind

direction and will have a radius (r_{acc}) as below,

$$r_{acc} \sim \frac{2GM}{v_{rel}^2} \tag{1.9}$$

where M is the mass of the compact object. The fraction of the mass captured by the compact object from the stellar wind of the companion is,

$$\frac{\dot{M}}{-\dot{M}_w} \cong \frac{\pi r_{acc}^2}{4^2} \cong \frac{1}{4}\left(\frac{M}{M_s}\right)^2\left(\frac{R_s}{a}\right)^2 \tag{1.10}$$

where $\dot{M}_W$ and $\dot{M}$ are the rate at which companion losses its mass and is captured by the companion respectively and a is the binary separation. For the typical values of the masses of the compact objects and star, radius of the star and binary separation this fraction is about 10^{-3}-10^{-4} (Frank *et al.*, 1992). Thus the fraction of the mass captured from the stellar wind is very small and seems like wind accretion inefficient compared to Roche lobe overflow but the rate of mass loss by a star in form of the stellar wind is very large because of which the sources appears luminous. The luminosity of the source in terms of $\dot{M}$ and $\dot{M}_w$ can be written as,

$$L \sim 10^{37}\left(\frac{\dot{M}}{10^{-4}\dot{M}_w}\right)\left(\frac{\dot{M}_w}{10^{-5}M_\odot yr^{-1}}\right). \tag{1.11}$$

A bow shock wave is formed at a distance r_{acc} from the neutron star due to accretion of highly supersonic stellar wind (see Fig. 1.3). Due to focusing of stellar wind an accretion disk is also formed behind the compact object. In HMXBs an accretion disk is formed if the accreting matter has some angular momentum and the circularization radius R_{cir}^w is greater than radius of the compact object. The R_{cir}^w is defined as,

$$R_{cir}^w \cong 1.3 \times 10^6 M_c^{1/3} P_{10}^{2/3} \tag{1.12}$$

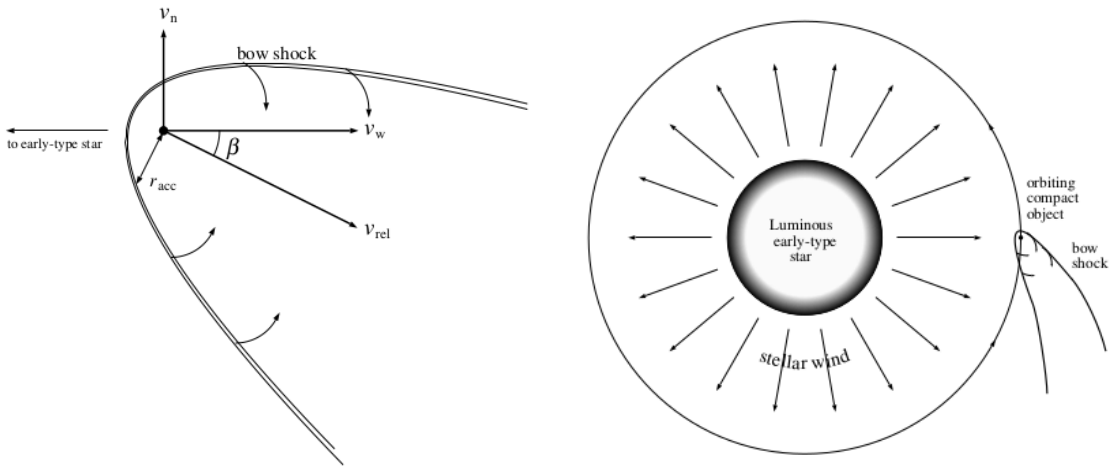

Fig. 1.3 Left: Schematic diagram of a compact object accreting matter through stellar wind. Right: Figure showing the direction of velocities of neutron star and wind.

where P_{10} is the orbital period in the unit of 10 days. However the formation of accretion disk is very rare in the case of HMXBs.

1.4.3 Be-disk Accretion

More than 60% of the HMXBs discovered are Be/X-ray binaries. One of the binary component of this system is an optical Be star, which is non-supergiant B-type star of luminosity class between III-V. The qualifier "e" denotes that spectral lines are observed in the spectrum of the star during some phase of its life which distinguished it from a normal B-star. The prominent spectral lines observed in Be stars are Balmar and Paschen series of the hydrogen but in some cases He and Fe lines are also found to emit (Reig, 2011). These stars also show large IR radiation than from B-star of same spectral type. The presence of the equatorial disk (Fig. 1.4) in BeXBs may be the reason for the origin of the emission lines and the infrared excess observed in the source. However the process through which this disc formed is not known yet but it is proposed that a rapidly rotating Be star expels matter forming the disk (Porter and Rivinius, 2003). The Be stars of the BeXBs are within the Roche lobe as the orbital periods of the system is very long and a

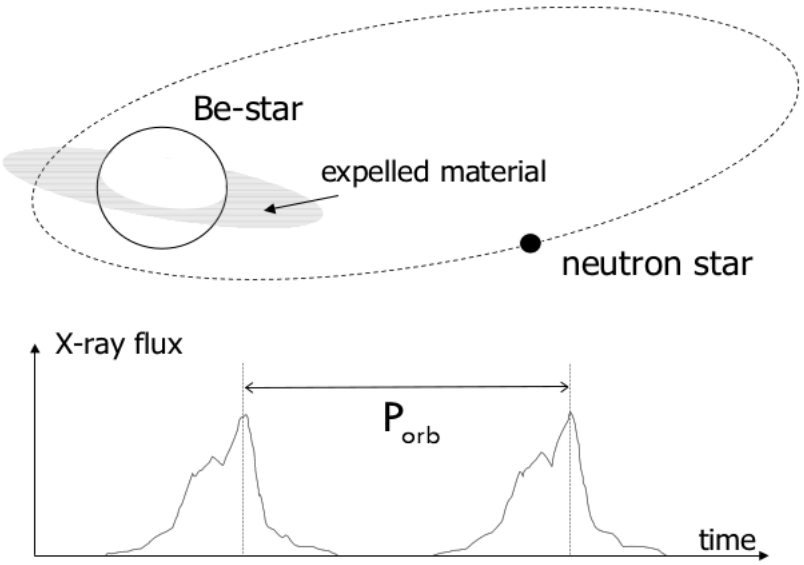

Fig. 1.4 Illustration of Be/X-ray binary system. The shadow near the Be star represents equatorial disk. The neutron star orbiting around the Be star captures matter from the disc during periastron passage and causes periodic outburst of type I. Image courtesy: (Tauris and van den Heuvel, 2006).

Be star being a non-supergiant. Mass is accreted by the neutron star in this system during periastron when the neutron star passage close to or through the equatorial disc of the Be star. The mass transfer occurs through the Roche lobe overflow. Due to accretion of large amount of materials during periastron passage a giant X-ray outburst is observed in these systems. BeXBs have a eccentric orbit with e$\geq$0.3 and orbital period in $\sim$13-330 days range.

BeXBs are mostly transient in nature which are observable only during an outburst. The outburst are of two types - Type I and Type II. Type I outburst are frequent and periodic in nature and occurs during periastron passage of the neutron star. The outburst last about 0.2-0.3 P_{orb} days, where P_{orb} is the binary orbital period. The luminosities during Type I bursts are found to be below Eddington limit reaching a peak value $L \leq 10^{37}$ erg s^{-1}. As compared to a Type I outbursts, the Type II outbursts are rare and giant. The luminosities during Type II outburst can reach or even cross the Eddington limit. These outbursts last

longer than Type I outburst and last for a large fraction of the binary orbital period or even cover few orbital periods. This type of outburst is not dependent on orbital phases. It is believed that an accretion disk is formed during the outburst which is also supported by the observations of quasi-periodic oscillations (QPOs) in some BeXBs. The steady spin-up rates in BeXBs during these outbursts are also explained by the presence of accretion disk. The reason behind those outbursts are yet to be known.

1.5 Neutron star X-ray binaries and X-ray pulsars

X-ray binaries consist of neutron star as a compact object. Neutron stars in X-ray binaries can have magnetic field about 10^8-10^{13} G. The presence of large magnetic field of the neutron star will affect the accretion of matter onto it. At certain radius disruption of the accretion flow occurs due magnetic field and accreted matter is then channeled by the magnetic field onto the magnetic poles of the neutron star. If we consider the magnetic field (B) of the neutron star to be a dipolar in nature then,

$$B \sim \frac{\mu}{R^3} \tag{1.13}$$

where μ is the magnetic dipole moment and R is the radius of the neutron star. The Alfven radius R_A is then defined as the radius at which the magnetic pressure $\frac{B^2}{8\pi}$ becomes equal to the ram pressure of the infalling matter given by $\frac{1}{2}\rho v^2$. Thus at R_A we have,

$$\frac{B^2}{8\pi} = \frac{1}{2}\rho v^2 \tag{1.14}$$

v is the velocity of the matter and for radial free fall in spherical geometry $v = \sqrt{2GM/R}$ and also $\rho = \dot{M}/4\pi vR^2$. Thus from above equation,

$$R_A = \left(\frac{\mu^4}{2GM\dot{M}^2}\right)^{1/7} = 3.2 \times 10^8 \, \dot{M}_{17}{}^{-2/7} \mu_{30}^{4/7} \left(\frac{M}{M_\odot}\right)^{-1/7} cm. \tag{1.15}$$

where $M_\odot$ is the solar mass, $\dot{M}_{17}$ is the mass accretion rate in the unit of 10^{17} gm s^{-1} and μ is in the unit of 10^{30} G cm^3. The Alfven radius is also called magnetospheric radius, for a distance smaller than this radius, the magnetic field will affect the flow of the infalling matter. The magnetosphere rotates with the same angular velocity as that of the neutron star. For non-spherical geometry the magnetospheric radius is bit modified. The accretion of matter depends on another quantity called co-rotation radius r_{co} which is defined as the radius at which the centrifugal force due to rotation of the neutron star magnetosphere counter balance the gravitational force acting on the accreting matter or in other words it is the radius at which the Keplerian frequency of the disk equals the neutron star spin frequency. Thus r_{co} can be expressed as

$$r_{co} = \left(\frac{GM}{\omega^3}\right)^{1/3}. \tag{1.16}$$

If $r_{co} > r_m$ then the centrifugal force due to rotation of magnetosphere becomes smaller than the gravitational force and there is an accretion of matter onto the neutron star. In this case the Keplerian velocity of the accreting matter is greater than the magnetospheric rotational velocity. The accreting matter is channeled by magnetic field along the neutron star poles. Depending upon the mass accretion rate $\dot{M}$ the accreting matter falling onto the poles is stopped either by radiative shock wave or Coulomb interactions. This causes accumulation of matter on the poles forming an accretion column of cylindrical shape. X-rays are radiated from the accretion column or accretion funnel. However, if $r_{co} < r_m$

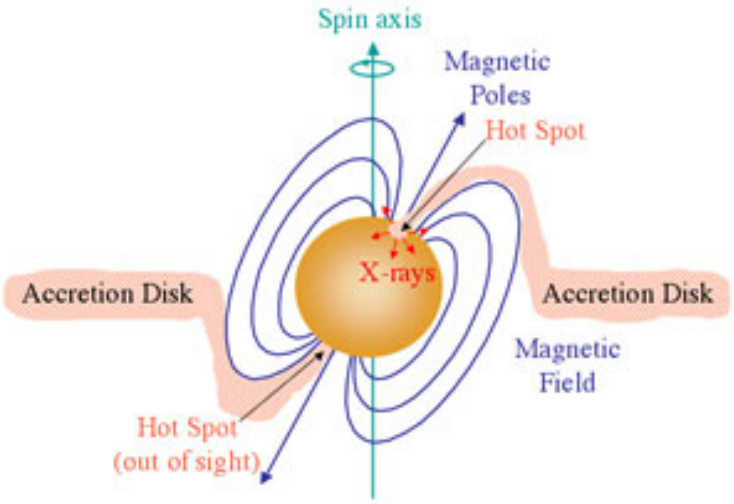

Fig. 1.5 Figure showing the accretion powered X-ray pulsar where matter is channeled along the magnetic field lines. The accretion columns are formed inside the the hot spots. Image courtesy : https://astronomy.swin.edu.au/cosmos/X/X-ray+Pulsar

then there exist a centrifugal barrier which prevents the accretion of matter onto the neutron star. This phenomenon of centrifugal inhibition is known as *propeller effect*.

The accretion columns formed at the magnetic poles of a neutron star emits X-rays through different mechanisms. If there exist misalignment between the magnetic axis and rotational axis (Fig. 1.5), then the X-rays emitted from the poles of the rotating neutron will appear as X-ray pulses. Hence the name X-ray pulsars, which are neutron star X-ray binaries that are powered by the accretion. The kinetic energy of the accreting matter moving with the velocity close to that of the light is released as radiation from the poles. The size of the accretion column is about $\sim$1 km (Davidson and Ostriker, 1973). However the shape and size of the accretion column along with the physical process behind its formation is not known completely. The emission geometry and the interaction of accreting matter with neutron star surface is determined by the mass accretion rate or the luminosity of the X-rays emitted by the pulsar. When the accretion rate is low thermal X-rays are emitted from the hot spots formed at the poles of the neutron star. However, for a large accretion rate a radiation dominated shock wavefront is formed above the neutron star's

poles. X-ray emission in this case occurs through the shock wavefront and the thermal mound at the bottom of accretion column through thermal and bulk Comptonization processes.

Based upon the luminosity of the pulsar Basko and Sunyaev (1976) proposed two types of accretion regimes. Those regimes were differentiated by a certain value of luminosity called critical luminosity (L_{crit}). If the luminosity of the X-ray pulsars is less than L_{crit} then the pulsars are said to be in sub-critical regime of accretion. For the luminosity greater than L_{crit} the source is in super-critical accretion regime. The critical luminosity depends on the magnetic field of the pulsar and the geometry of accretion disk (Becker *et al.*, 2012). Becker *et al.* (2012) considering the different physical processes that are occurring in the accretion column determined the critical luminosity for X-ray pulsars having cyclotron absorption feature in their spectra, which is given by

$$L_{crit} = 1.49 \times 10^{37}_{0.1}{}^{-7/5} w^{-28/15} M_{1.4}^{29/30} R_{10}^{1/10} B_{12}^{16/15} ergs^{-1} \tag{1.17}$$

where $M_{1.4}$ is the mass of the neutron star in the unit of $1.4M_{\odot}$, R_{10} is the radius of the neutron star in the unit of 10 km and B_{12} is the magnetic field in the unit of 10^{12} G. Λ is a constant which is considered 1 for a spherical accretion but it is less than 1 for a disk accretion. The parameter w lies between $1-3$, $w=1$ corresponds to Bremsstrahlung spectrum whereas for $w=3$ corresponds to Planck spectrum. Considering the typical value of neutron star parameters *i.e.* $M_{1.4}=1$, $R_{10}=1$, $\Lambda=0.1$ and $w=1$, the critical luminosity becomes,

$$L_{crit} = 1.49 \times 10^{37} B_{12}^{16/15} erg\ s^{-1} \tag{1.18}$$

For low mass accretion rate the X-ray luminosity is smaller than the critical luminosity ($L \ll L_{crit}$). In this case there exist two zone in the accretion column - free falling zone and

shock zone. In free falling zone matter falls freely until it encounters shock near the surface of the neutron star (Basko and Sunyaev, 1976). In the shock zone the deceleration of matter takes place through electrostatic interaction. The X-rays from the hot spot escapes vertically upward along the accretion column. As a result pencil-beam emission pattern is formed which is shown in Fig. 1.6.

A different scenario of accretion formed when the luminosity is close to or equal to the critical luminosity ($L \leq L_{crit}$), in this case the radiation dominated shock wave is formed in the accretion column (Fig. 1.6). Radiation from the accretion column below the shock region is emitted along the direction perpendicular to the column as a result a fan-beam shaped emission pattern is found whereas the radiation above the shock region moves upward in the form of a pencil beam pattern. Thus the resulting beaming pattern is a mixture of pencil and fan beams. Below the shock the plasma is decelerated by electrostatic interaction that sinks slowly toward the neutron star.

For a high accretion rate the luminosity of the source is higher which is greater than the critical luminosity ($L > L_{crit}$), in this case the accreting matter is completely halted by the radiation dominated shock and loses all of its kinetic energy. The shock rises above the surface of the neutron star with an increase in accretion rate and beneath the shock region there exists an extended sinking zone (Basko and Sunyaev, 1976). In this case X-ray emission results only along the side walls of the accretion column and we get a pure fan-beam emission pattern.

1.5.1 Accretion X-ray millisecond pulsars

Accretion X-ray millisecond pulsars (AMXPs) is a subclass of LMXBs which are rotating very fast about few hundreds of times in one second. Soon after the discovery of first millisecond radio pulsar in 1982 (Backer *et al.*, 1982), it was believed that LMXBs are the progenitor of the millisecond radio pulsar. It was suggested that during the course of

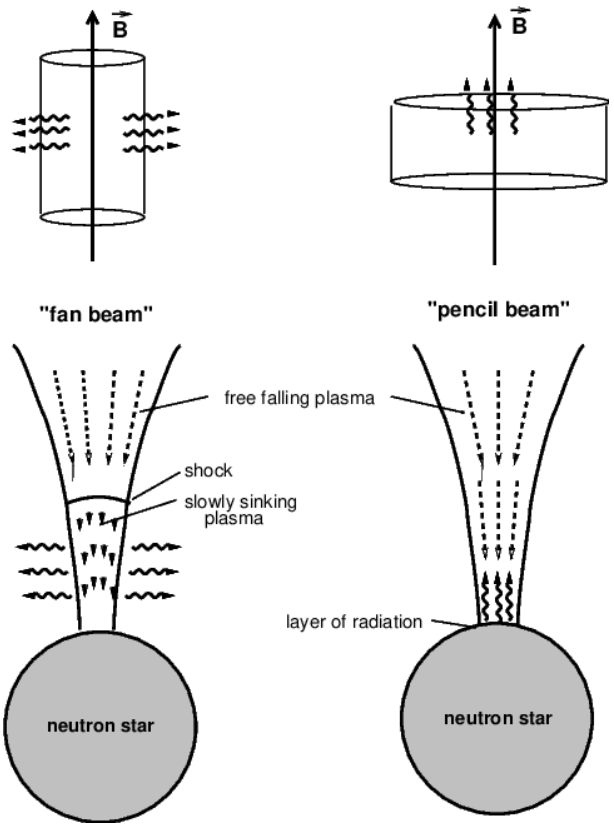

Fig. 1.6 The figure on the left represent the super-critical accretion regime where matters fall freely until it encounters a shock above the neutron star surface. From the region below the shock X-rays are emitted in the direction perpendicular to the accretion column to produce fan beam. The figure on the right hand side is in case of luminosity below the critical value. In this case X-ray escapes vertically upward from the hot spots along the accretion column to produce pencil beam pattern. Image courtesy - Schönherr *et al.* (2007)

evolution of LMXBs the slow rotating neutron stars evolves into the fast rotating neutron stars. The mechanism responsible for the spinning-up of the pulsar is the transfer of angular momentum due to accretion of matter from the companion to the neutron star (Alpar *et al.*, 1982; Radhakrishnan and Srinivasan, 1982). The formation of accreting millisecond X-ray pulsar is explained by what is known as "recycling scenario". A radio pulsar stops emitting radio pulsation after entering a phase called "pulsar-graveyard". After entering this phase the neutron star in a binary with low mass non-collapsed companion be such that during the evolution of the binary system the companion comes in contact with the neutron star through Roche lobe and the transfer of mass from companion to the neutron star occurs. In

addition to transfer of mass there is also a transfer of large amount of angular momentum onto the neutron star resulting in the enhancement of accretion torque which spin-up it. So in a broad sense there is recycling of radio pulsars to AMXPs and hence the name "recycling scenario". At the end when transfer of mass from companion stops the neutron star can no longer emits X-rays but can emit radio waves as recycled millisecond radio pulsar.

The first AMXP discovered was SAX J1808.4-3658 in 1998 by *Rossi X-ray Timing Explorer (RXTE)* (Wijnands and van der Klis, 1998) and provided confirmation of the recycling scenario. Another confirmation of this scenario came through the discovery of a radio millisecond pulsar PSR J1023+0038 with an accretion disk (Archibald and Stairs, 2009). This was the first observed case where a neutron star transforms to a radio pulsar after the X-ray pulsar phase of the star. The model is further supported by the discovery of the millisecond pulsar IGR J18245-2452 (Papitto and Ferrigno, 2013) which shows both an AMXP and radio millisecond pulsar phase. Till date there are 20 AMXPs (Salvo and Sanna, 2020) discovered. Some AMXPs are ultra compact binary systems between neutron star and white dwarf with an orbital period (P_{orb}) less than or equal to 80 min. For compact systems the neutron star companion is a brown dwarf which has an orbital period between 1.5-3 hr. However for wider systems of binary pulsars, the companion may be normal main sequence star with orbital periods between 3.5-20 hr. AMXBs are transient in nature which can be observed during an outburst. Most of the AMXBs have shown only one outburst after their discovery but few of them show recurrent outbursts. The outbursts in most cases last from few days to about three months. NGC 6440 X-2 has shown a recurrence time of one month which is the shortest recurrence time of the outburst observed in AMXPs. The longest duration of an outburst was observed in HETE J1900.1-2455, which lasted for 10 years.

It is known that intermittency of the pulsations can be observed also in AMXPs. This phenomenon was first observed in the AMXP HETE J1900.1-2455 during 2005 outburst when pulsation of 377 Hz was observed during the first 20 days of the outburst and thereafter went in the intermittent phase for next 2.5 years and after that there were appearance and disappearance of pulsations in various instances (Galloway *et al.*, 2007). Another case of intermittency of the pulsation is found in AMXP Aql X-1 where the coherent pulsation is detected only in 150 s data segment with a total exposure time of 1.5 Ms. This phenomenon is particularly important in understanding the absence of pulsations in the major fraction of NS LMXBs. SAX J1748.9-2021 also shows intermittency in pulsation where pulsation is observed in several data segments and it is observed that in three out of four outbursts (Altamirano *et al.*, 2008; Patruno *et al.*, 2009a). This phenomenon is particularly important in understanding the absence of pulsation in the major fraction of the observed time of NS LMXBs. Intermittency in the system is thought to be due to decrease in the magnetic field strength by three order of magnitude on a timescale of few hundreds of days which does not allow disk to truncate and in this case a very small fraction of gas is channeled producing weak pulsation (Patruno and Watts, 2013). However the theory proposed by Patruno and Watts (2013) is not complete and it cannot explain all the phenomenology that are observed in AMXPs.

During an outburst AMXPs have luminosity less than 10% of the Eddington limit and no transition from hard to soft spectral states is observed. The spectral state of AMXPs is similar to that of the NS LMXBs in hard state. The X-ray continuum of AMXPs consist of one or more blackbody components and a Comptonization component having cutoff energies of tens of keV. In few AMXPs florescence iron lines are observed in the 6.4-6.7 keV energy range which however are found to smeared out by the Doppler and relativistic effect. In some AMXPs X-ray photons are scattered in the disk producing excess of emission between 10-30 keV which is known as Compton hump (Papitto *et al.*, 2010).

They have long term spin down rate of 10^{-15}-10^{-16} Hzs^{-1}. The spin down of AMXPs are likely caused by the loss of angular momentum in the form of magnetic dipole radiation which can be used to constraint the magnetic field of the neutron star in AMXP with magnetic field of the order of 10^8 G.

1.6 Generation of X-rays in Astrophysics

It is known that there are four main processes through which continuous X-rays are produced. These are as follows,

- **Blackbody emission** - A body which absorbs radiation emits radiation. The energy of the emitted photon depends on the temperature of the body. A hot body which is above absolute zero temperature emits electromagnetic radiation. So stars can also radiates it energy in the form of electromagnetic radiation like blackbodies. Newly formed neutron stars or hots spot of accretion powered X-ray pulsars which can have a temperature of the order of 10^6 K emits X-rays in the form of blackbody radiation.

- **Bremsstrahlung** - Most of the matters are in the plasma state at a temperature above 10^5 K, so the gas consists of positively charged ions and electrons. These charged particles are also in thermal equilibrium. During a close interaction between an electron and a positive ion, due to strong electric force the electron gets accelerated. This accelerated electron then radiates electromagnetic radiation which is known as Bremsstrahlung (braking radiation). The emitted electromagnetic radiation of electron has continuum shape which depends only on the temperature. With the increase in the temperature the velocity of electrons increases which means that their energy also increase, so energy of radiation emitted by Bremsstrahlung process also increases. At temperature above 10^6 K, photons emitted lies in the X-ray range.

- **Synchrotron radiation** - In the presence of a magnetic field a fast moving electron changes its direction of motion as the field exerts Lorentz force perpendicular to the direction of motion. The change in the velocity the electron is associated with acceleration of electron resulting in emission of electromagnetic radiation. This type of radiation is known as magnetic Bremsstrhlung or synchrotron radiation. The frequency of the emitted radiation depends both on the magnetic field and the energy of the electron. The existence of synchrotron radiation indicates the presence of relativistic electrons as one observes in the synchrotron radiation from a radio emitting shell-like supernova remnants where the energy of the electrons emitting radio waves are about 1 GeV.

- **Inverse Compton scattering** - When low energy photons are scattered by ultra relativistic electrons then photons will gain energy from the relativistic electron, which is the inverse of Compton effect. This process is called inverse Compton effect. For a photon having an energy $h\nu$, the relativistic energy of the scattered photon is $\gamma^2 h\nu$, where $\gamma = \sqrt{1 - \frac{v^2}{c^2}}$ represents the Lorentz factor for electron moving with velocity v which is comparable to the velocity of light c. Thus even a photon of few eV can be scattered by ultra relativistic electron to produce X-ray or γ-ray photon by this process.

The blackbody emission and Bremsstrahlung are the thermal processes where as Synchrotron and inverse Compton scattering are the non-thermal processes that are responsible for the origin of X-rays in the neutron star. Apart from the continuous X-rays spectrum there might exist a discrete X-ray spectrum. This discrete X-ray spectrum is due to the characteristic X-rays.

1.6.1 Characteristic X-rays

The characteristic X-rays appears as sharp peaks in the continuous X-ray spectrum. In principle the de-excitation of excited atoms or ions occurs by the emission of photons which appears as emission lines. There is two main process through which the characteristic X-rays are produced - (1) Fluorescence and (2) Recombination.

1. **Fluorescence** - When a highly energetic X-ray photons hit atoms it can knock the electrons from the inner most orbitals. Electrons from high energy orbitals fills the vacancy so created and the resulting photons having energy equal to the energy difference between two orbitals is emitted. This gives us the fluorescent X-ray lines. The well observed fluorescent X-ray lines in the spectrum of X-ray binaries that of neutral or ionized iron in 6-7 keV energy range.

2. **Recombination lines** - These spectral lines are observed during ion-electron recombination. The recombination of electron with ion usually leaves the ion in an excited state. This excited ion emits photons as the electron jumps successively into the lower energy states and finally to its normal stable state.

1.7 X-ray spectra

X-ray spectra of X-ray binaries (XRB) are almost continuous in shape and which is described by a power law having cutoff energy in 10-30 keV energy range. In some cases there will be blackbody component in soft X-ray range *i.e.* below 5 keV. Along with the continuum shape there exist fluorescence emission lines of iron and other elements in some cases. In some accretion powered X-ray pulsars absorption like feature which is known as cyclotron resonance scattering features (CRSF) are also observed. Although the physical processes responsible for the generation of X-rays in accretion column and in magnetosphere are very complex but the spectra are found to be well predicted by

phenomenological models. It is found that models which fits the spectrum of one XRB well does not fit the other XRBs satisfactorily. There have been several attempts to produce the spectra theoretically (Nagel (1981), Meszaros *et al.* (1983), Burnard *et al.* (1991)) but due to the complexity of the processes a standard model that defines the spectra of X-ray binaries is not known satisfactorily. The absence of knowledge of precise geometry of the accretion column further increases this complexity. The theoretical model proposed by Becker and Wolff (2007) was successful in explaining the continuum shape of Her X-1, LMC X-4 and Cen X-3. This model is based on the bulk and thermal Comptonization of X-ray photons in the accretion column. The fig. 1.7 shows the theoretical spectrum of LMC X-4. Schematically this model is described in fig. 1.8. Soft photons generated by blackbody radiation at the thermal mound located at the bottom of the accretion column act as seed photons for upscattering. The optically thin region above the thermal mound produces bremsstrahlung and cyclotron photons. These photons move upward in the radiation dominated shock in the accretion column and gets upscattered by the electrons in the gas by the process of bulk Comptonization. The thermal Comptonization of photons is responsible for the cut-off and flat soft X-ray spectrum. Another theoretical model COMPMAG (Farinelli *et al.* (2012, 2016)) generally useful for the description of the spectral formation based on the bulk and thermal Comptonization of the photon.

1.7.1 Cyclotron Resonance Scattering Feature

In the spectra of X-ray pulsars the Cyclotron Resonance Scattering Feature (CRSF) which are commonly known as cyclotron lines are observed as absorption like feature in between 10-100 keV energy range. The feature was first observed in Her X-1 (Trümper *et al.*, 1978). The physical mechanism responsible for the cyclotron resonance is the resonant scattering of the X-ray photons by quantized electrons on the surface of the neutron star. These electrons have energy state in the quantized Landau levels. This feature is directly related

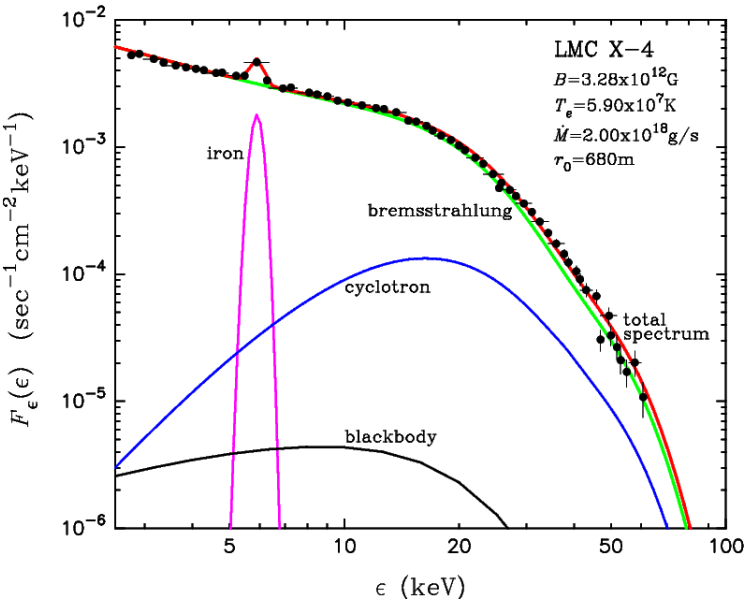

Fig. 1.7 Theoretical spectrum of LMC X-4 computed by Becker and Wolff (2007)

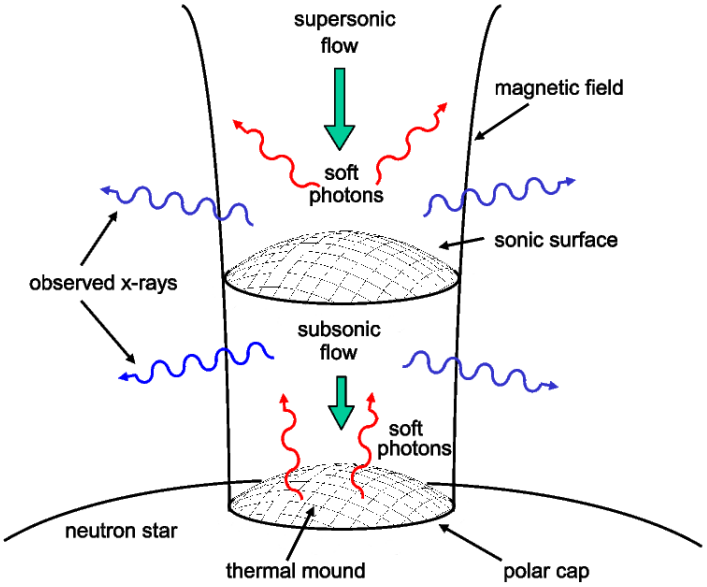

Fig. 1.8 An illustration of accretion column of accreting neutron star. Seed photons are produced through blackbody at the thermal mound at the base of the accretion column where as seed photons through bremmstrahlung and cyclotron are produced throughout the accretion column. Image courtesy Becker and Wolff (2007)

to the magnetic field of the neutron star and the presence of this feature in the spectra of pulsars helps us to estimate the magnetic field of the neutron star.

The origin of the cyclotron line can be explained by quantum electrodynamics. The trajectory of the electrons follows helical path due to the Lorentz force in the presence of magnetic field. The electrons revolves in the helical trajectory with a frequency known as Larmor frequency. The Larmor frequency (ω_b) and radius (r_b) are given by,

$$\omega_b = \frac{eB}{m_e c}, \tag{1.19}$$

$$r_b = \frac{m_e v_\perp}{eB} \tag{1.20}$$

where m_e is the mass of the electron, $v_\perp$ is the perpendicular component of electron's velocity, e denotes the charge of an electron and B is the magnetic field of the neutron star. Thus the Larmor radius decreases as the magnetic field increases and once it approach the de-Broglie wavelength then the quantum mechanical effect become important for its description. The electron then gets quantized in the direction perpendicular to the magnetic field into the discrete Landau levels. For the Landau levels, the energy of an electron is given by,

$$E_n = \frac{mc^2}{sin^2\theta}\left(\sqrt{1+2n\frac{B}{B_{crit}}sin^2\theta} - 1\right) \tag{1.21}$$

where θ is the angle between the incident photon and the magnetic field, $B_{crit} = \frac{m_e^2 c^3}{e\hbar} \approx 4.4 \times 10^{13}$ G which is the critical magnetic field at which the kinetic energy of the electron or Landau's energy level becomes equal to the rest mass energy of the electron. Here n is a positive integer such that $n = 1$ corresponds to fundamental cyclotron line and that with $n = 2,3,4$ correspond to its harmonics. From eq. (1.21) it is evident that the line energy depends strongly on the angle θ. In case of strong gravitational field the above equation is modified by a factor $(1+z)^{-1}$, where z is redshift parameter. Thus the cyclotron line

corresponds to the internal geometry of the accretion column. When the magnetic field is greater than or equal to the critical B_{crit} *i.e.*B$_{crit}$ then the relativistic corrections of path of the electron moving in the magnetic field becomes important (Araya-G'ochez and Harding, 2000). In the non-relativistic case when the magnetic field is very small compared to the critical value B_{crit} i.e. $B << B_{crit}$, then the energy difference between the quantized states is given by

$$E_{cyc} = \hbar\omega_b = \frac{e\hbar}{m_e c}B = 11.6B_{12}\ keV \tag{1.22}$$

where B_{12} is the magnetic field in the order 10^{12}G. In the presence of strong gravitational field the above energy is to be modified by redshift correction term $(1+z)^{-1}E_{cyc}$. The above formula in eq. (1.22) is used to estimate the magnetic field of a neutron star for a known value of the cyclotron line energy. Thus in the presence of magnetic field the energy state of electrons are quantized at Landau levels, the photons having energy in the integral multiple of E_{cyc} are absorbed by these electrons. As a result electron gets excited and moves into the higher energy states of Landau levels. These states are very unstable with life time much shorter than that of the time scale of collision de-excitation of electrons. As a result re-emission of the absorbed photon of same energy occurs. Instead of absorption of photon the whole process can be considered as the resonant scattering. As there exist a continuity between absorption and emission processes in plasma, photons having energy in the integral multiple of E_{cyc} will get trapped in the accretion column region. During an inelastic scattering process the energy of these photons changes and it escape the accretion column at suitable energy. As a result of which broad absorption like features are observed in the spectra of X-ray pulsars at the energy close to an integral multiple of E_{cyc}. It is also observed that in some X-ray pulsars fundamental cyclotron line is associated with its harmonics in some cases. The variation of scattering of cross section with energy for exciting an electron in different Landau levels are shown in Fig. 1.9.

Gnedin and Sunyaev (1974) first theoretically demonstrated the presence of the cyclotron resonance scattering features (CRSF) even before the feature was actually discovered by observations. However the origin of this feature is not fully understood. There are three methods by which the formation of the feature can be simulated - (i) Monte Carlo (Araya and Harding, 1999; Araya-Góchez and Harding, 2000), (ii) Feautrier methods (Meszaros and Nagel, 1985) and (iii) analytically (Wang *et al.*, 1993). The Monte Carlo simulation of CRSF based on the interpolation table of mean free path of the scattering photon and the momentum of the scattering electron with a magnetic field B such that $0.01 \leq B/B_{crit} \leq 0.12$ and electron temperature lying between 3-15 keV was considered by Schwarm *et al.* (2017). This method can be used to simulate CRSF for X-ray pulsars having complex accretion geometry for a given magnetic field and viewing angles. The features depend on the geometry of the emission, plasma properties and on the optical depth of the column.

The cyclotron lines are modeled using either Gaussian or pseudo-Lorentzian profiles to obtain its line energy, equivalent width and the strength. The above parameters are found to vary with pulse phase and the luminosity. The line energies either shows correlation or anti-correlation with the luminosity. It has been shown (Basko and Sunyaev, 1976; Becker *et al.*, 2012) that this is because of two accretion regimes depending on the critical luminosity. At super-critical luminosity X-ray pulsars the emission pattern may be fan-shaped which affects the CSRF through Doppler effect on the observation of anti-correlation of CRSF with luminosity. In the sub-critical regime it is observed that the emission pattern is a pencil beam admitting positive correlation of CRSF with energy. However, there are some X-rays pulsars which do not show any correlation with the luminosity. In some cases a wings are observed in the fundamental cyclotron lines which are believed to be due to photon spawning effect.

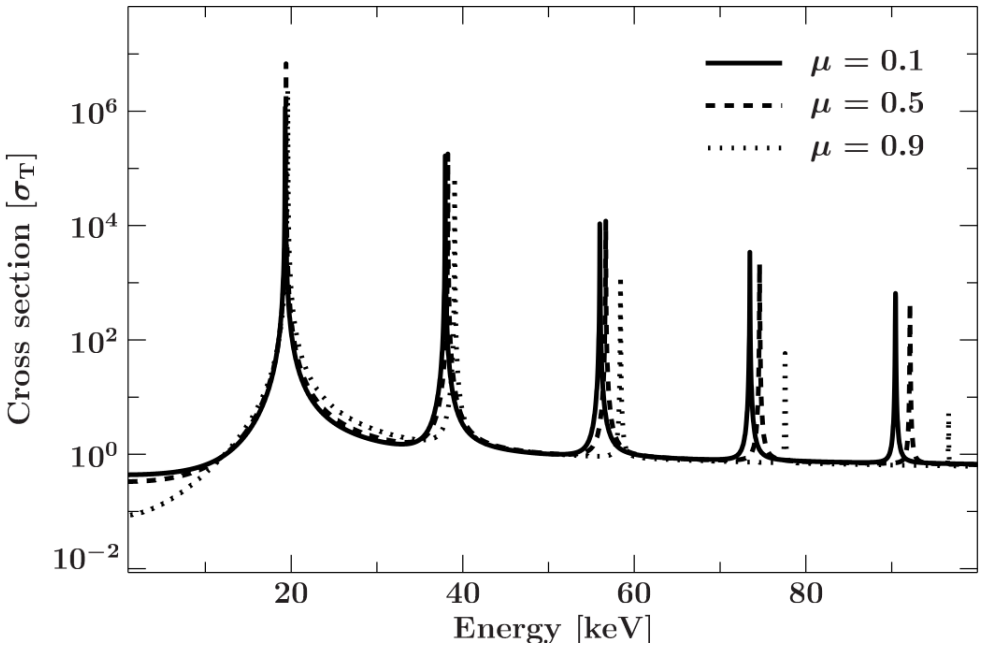

Fig. 1.9 Variation of scattering cross section with energy for exciting an electron in initial Landau level $n = 0$ to $n = 6$ for given magnetic field about $B = 0.0385 B_{crit}$. The fundamental cyclotron line is at 20 KeV. The solid, dashed and dotted lines represents cross section for three viewing angle $\nu = cos\ \mu = 0.1, 0.5, 0.9$ respectively. Figure courtesy-Schwarm *et al.* (2017).

1.8 Pulse Profiles

The temporal variation of the photon counts per unit time is called light curve. Light curves of X-ray pulsars show periodicity due to the rotation of the neutron stars. By folding these light curves about the spin period of the neutron stars pulse profiles are obtained. Pulse profile of a pulsar shows variation of the X-ray intensities with the pulse phases. Pulse profiles of different X-ray pulsars are different and unique.The shape of the pulse profiles depends on various factors like properties of the accretion column, emission geometry, mass accretion rate, angle between magnetic and rotational axes and bending of light due to gravitation. Considering the beam pattern along with the variation in the geometrical aspect of magnetic axis, geometric axis and the line of sight one can reproduce the pulse profiles. If α and β are the angle which the rotational axis makes with the magnetic axis and the line of sight respectively then both poles are visible if $\alpha + \beta > \pi/2$ and

only one visible if $\alpha + \beta < \pi/2$. A single peaked pulse profiles is thought to be due to emission from a single pole of the neutron star where as the double peaked pulse profiles are due the emission from two poles of the neutron star. In some pulsars multiple peaks are also observed in the soft X-ray energy range. In some cases dips are also observed in pulse profiles at some specific phases this might be due to the eclipsing of the radiation emitted from the hotspot by an optically thick plasma in the accretion column (Cemeljic and Bulik, 1998). It has been observed that at the phases close to the dip the spectrum varies significantly with a large variation in the optical depth, it may be because of an extension of the accretion column only along a direction in these phases (Galloway *et al.*, 2001; Giles *et al.*, 2000). An alternate explanation of the dips is that during these phases the accretion stream comes between the hot spot and our line of sight (Maitra and Paul, 2011; Naik *et al.*, 2011). In some pulsars dips disappear in hard X-ray range. However depending on the density and opacity of matter in accretion column or streams, the dips may be observed at higher energies too. In some pulsars a phase reversal of 180 degree is observed as one moves from soft to hard X-rays range (Beri *et al.*, 2014). It has also been observed that in some pulsars there is sudden change or shift in phase at an energy very close to the cyclotron line energy. Studies of the cyclotron line energy based on the numerical simulations have found that the presence of strong absorption feature due of CSRF can affect the emission of the X-ray beam. Hence the change in pulse profiles are observed at an energy close to the cyclotron line energy (Schönherr *et al.*, 2014).

The X-ray pulsars in which the mass accretion rate and hence the luminosity varies throughout an outburst, the pulse profile is complex in the case where luminosity is above the critical value as a radiative shock wave is formed few kilometers above the neutron star as discussed earlier. If the luminosity is below the critical luminosity then the pencil beam pattern produces a simple pulse profile which is more or less sinusoidal in shape.

1.9 Objective of the thesis

The objective of the thesis is to investigate some of the salient features of neutron star X-ray binaries. The pulse profiles of the star which depends on the mass accretion rate, geometry of accretion disk, magnetic field and its distribution around the neutron star will be studied. The cyclotron lines present in the spectrum of these binaries are the direct source of information of the presence of magnetic field in the source will be use to estimate the magnetic field of the neutron star. To understand the surrounding environment of the neutron star the pulse phase-resolved spectroscopy will be used. The origin of flares in the light curves of some of the X-ray binaries are also analyzed. For the analysis the following types of sources namely, NS LMXB (AMXB) and HMXBs (SGXB & BeXB) are taken up.